Annals of Arid Zone 65(4): 103-121, 2026

Remote Sensing Evidence of Climate-Driven Vegetation Decline and Desertification in the Biskra Region Northeastern Algeria (2005-2025)

S. Abbas and N. Diab*

Scientific and Technical Research Center on Arid Regions CRSTRA, P.O. Box 1682, Rp 07000. Biskra, Algeria

Received: January 21, 2026 Accepted: March 23, 2026

Abstract: Arid and semi-arid regions are particularly vulnerable to climate change, where rising temperatures and declining rainfall accelerate vegetation degradation and desertification processes. Remote sensing provides an effective framework for monitoring these environmental changes over time. This study aims to assess spatio-temporal vegetation dynamics and identify the role of climate change in driving desertification in the Biskra region between 2005 and 2025, using multiple remote sensing vegetation indices. The findings reveal significant environmental degradation in the Biskra region over the study period. The median Green Chlorophyll Index (GCI) declined sharply from 1.5 to 0.78, indicating a marked reduction in photosynthetic efficiency. Similarly, the median Enhanced Vegetation Index (EVI) decreased from 0.4 to 0.1, reflecting severe vegetation stress. The Transformed Soil-adjusted Vegetation Index (TSAVI) showed a 35% loss in peak vegetation density between 2005 and 2015, with its maximum value dropping from 0.94 to 0.61. Although a partial recovery was observed by 2025, as the TSAVI maximum returned to 0.94, this improvement remained localized and did not represent a regional recovery. These vegetation declines coincided with pronounced climatic changes. Mean annual temperature increased from 20.5°C to 23.8°C, while precipitation became increasingly irregular, decreasing from 152 mm to 118 mm and reaching a critical minimum of 68 mm during the 2021 drought. Additional indices confirmed the degradation trend, with median NDVI values falling from 0.15 to 0.08 and SAVI from 0.18 to 0.09. Spatial analysis revealed persistent heterogeneity, with high-density vegetation confined to northern areas, while degraded zones expanded to cover 78% of the region. Overall, the results highlight climate change as the primary driver of desertification, emphasizing the urgent need for targeted ecosystem resilience strategies.

Key words: Multi-index, degradation, climate change, remote sensing, arid regions, spatio-temporal analysis.

OPEN ACCESS

Editor-in-Chief
Praveen Kumar

Editors (India)
Anita Pandey
Hema Yadav
Neena Singla
Ritu Mawar
Sanjana Reddy
Surendra Poonia
R.K. Solanki
P.S. Khapte

Editors (International)
M. Faci, Algeria
M. Janmohammadi, Iran

***Correspondence**
N. Diab
diab_nassima@yahoo.fr

Citation
Abbas, S. and Diab, N. 2026. Remote sensing evidence of climate-driven vegetation decline and desertification in the Biskra region northeastern Algeria (2005-2025). Annals of Arid Zone 65(4): 103-121

https://doi.org/10.56093/aaz.v65i4.175417

https://epubs.icar.org.in/index.php/AAZ/article/view/175417

Vegetation cover degradation is a major ecological challenge, characterized by persistent declines in vegetation

© 2026: Licensed under the Creative Commons Attribution-NonCommercial-ShareAlike 4.0 International License (CC BY-NC-SA 4.0)

and substantial biodiversity losses over recent decades (Encinas-Valero *et al*., 2022; Deghiche-Diab, 2020; Aouissi *et al*., 2021; Reynolds *et al*., 2007; Maestre *et al*., 2022). This degradation is further exacerbated by climate variability, soil degradation, and anthropogenic pressures, including deforestation, overgrazing, and unsustainable land-use practices. Together, these interacting factors accelerate ecosystem degradation, reduce biodiversity, and undermine vegetation's resilience and capacity to recover from environmental disturbances (Lambin *et al*., 2001; Geist and Lambin, 2004; IPCC, 2021). Arid and semi-arid regions are undergoing significant climatic changes that profoundly disrupt Saharan ecosystems in particular. These changes manifest through thermal anomalies, shifts in precipitation patterns, and an increase in the frequency of extreme events, such as prolonged droughts. These eco-physiological disturbances lead to increased water stress, a decrease in photosynthesis, and reduced plant growth. As a result, the biogeographical ranges of plant species are shifting, in some cases toward less suitable habitats, thereby further weakening ecosystem stability and resilience (Parmesan and Yohe, 2003; Chen *et al*., 2011).

Consequently, desertification is intensifying, and the ecological niches of native arid-adapted species are being disrupted, often leading to a loss of biodiversity and the invasion of non-native species, which further destabilizes these fragile ecosystems (Maestre *et al*., 2022; Deghiche-Diab *et al*., 2023). This process accelerates land degradation, critically impairing the capacity of these landscapes to recover and sustain their vital ecological roles, such as soil stabilization, nutrient cycling, and the support of pastoral and agricultural livelihoods (IPBES, 2018; Bai *et al*., 2008). This dynamic further intensifies vegetation degradation, thereby compromising the capacity of ecosystems to regenerate and perform essential ecological functions, including carbon sequestration, soil protection, and the regulation of hydrological cycles (Berdugo *et al*., 2020). To understand the interaction between these degradation factors and climate impacts, the application of remote sensing is an effective and economical method. This technique allows for regular monitoring, precise mapping, and temporal analysis of changes at various spatial scales (Turner *et al*., 2015; Gorelick *et al*., 2017). Data from Landsat satellites, particularly those from Landsat-5 and 8, stand out for their high spectral resolution and free accessibility, making them a valuable tool for vegetation research at the global, continental, regional, and national levels (Roy *et al*., 2014; Wulder *et al*., 2018; Zhu *et al*., 2020).

Remote sensing, based on the interaction between radiative energy and matter, facilitates continuous and repeated monitoring of vegetation cover. It allows for the detection of temporal variations, the analysis of time series, and the revelation of patterns related to phenology, vegetation growth, seasonal fluctuations, and long-term trends (Pettorelli *et al*., 2018; Zhu *et al*., 2016). This information is crucial for understanding ecosystem dynamics, detecting disturbances, and assessing the impacts of climate change (Turner *et al*., 2003; Fensholt *et al*., 2012). In this context, the present study focuses on the detailed mapping of vegetation cover in the arid regions (Biskra province), located in the northeast of the Algerian Sahara, over twenty years from 2005 to 2025. This study documents the spatio-temporal dynamics of forest cover using a suite of advanced vegetation indices.

The core indicators include the Normalized Difference Vegetation Index (NDVI), Soil-Adjusted Vegetation Index (SAVI), Modified SAVI (MSAVI), Transformed SAVI (TSAVI), Green Chlorophyll Index (GCI), and Enhanced Vegetation Index (EVI). NDVI assesses vegetation density and health, supporting biomass estimation and global ecosystem monitoring. SAVI and its variants (MSAVI, TSAVI) correct for soil brightness and local soil conditions, improving accuracy in sparse or arid environments. GCI measures chlorophyll content, reflecting photosynthetic activity and stress, while EVI further enhances sensitivity by correcting for atmospheric and canopy background effects, especially in high-biomass regions (Abbas, 2024). Integrating these vegetation indices into multispectral remote sensing data analysis enables a comprehensive assessment of vegetation health, density, and structural characteristics, providing an integrated understanding of vegetation ecological dynamics in Biskra Province. This approach is designed to support the identification and management of fragile areas and to inform conservation strategies

essential for the long-term preservation of the region. Beyond the spatio-temporal analysis, a central aim of this study is to jointly examine the relationships among the vegetation indices (NDVI, SAVI, MSAVI, TSAVI, GCI, and EVI). To this end, a correlation analysis is conducted to evaluate how these indices respond collectively or divergently to environmental conditions, to clarify their complementarity, individual sensitivity, and overall relevance for monitoring long-term vegetation dynamics.

Material and Methods

Study area

Geographically, Biskra Province (Fig. 1) is located in the northeastern part of the Algerian Sahara. It extends south-eastward towards the Chott Melghir area and south-westward to the beginning of the Great Eastern Erg, with an average altitude of approximately 124 m above sea level. It extends over an area of 10246 km^2 (Deghiche-Diab and Deghiche, 2022). It is bounded by Batna Province to the north, M'sila Province to the northwest, Khenchela Province to the east, Ouled Djellel Province to the southwest, and El Oued Province to the southeast and south, while El M'ghair Province also borders it to the south. The region is characterized by a diverse landscape, with mountainous terrain dominating the northern areas and gradually giving way to plains toward the south, ultimately extending into vast desert expanses interspersed with fertile oases.

Climatic Characteristics: Biskra Province, located in southeastern Algeria between latitudes 34°N and 35°N, lies at the interface between the Saharan and steppe bioclimatic zones. The region is characterized by a hot desert (arid to semi-arid) climate according to the Köppen classification (BWh–BSh) (Ozenda, 2004). Annual rainfall is low and irregular, averaging between 50 and 150 mm, concentrated mainly between November and March (ONM, 2022). Temperatures show strong seasonal and daily variations. Summer is extremely hot, with maximum temperatures often exceeding 45°C in July and August, while winter remains mild, with averages around 12 to 15°C and occasional drops below 5°C (IPCC, 2021; Hersbach *et al.*, 2020). The mean annual temperature is approximately 22 to 23°C. The region experiences high evapotranspiration rates and frequent hot winds (*chili* or *chergui*), which accentuate aridity and soil desiccation. Relative humidity rarely exceeds 40% during the dry season. The climatic regime also features short, intense rain events, leading to flash floods in the surrounding wadis such as Oued El Arab and Oued Mellah (Hamlât *et al.*, 2021). This extreme climatic variability directly

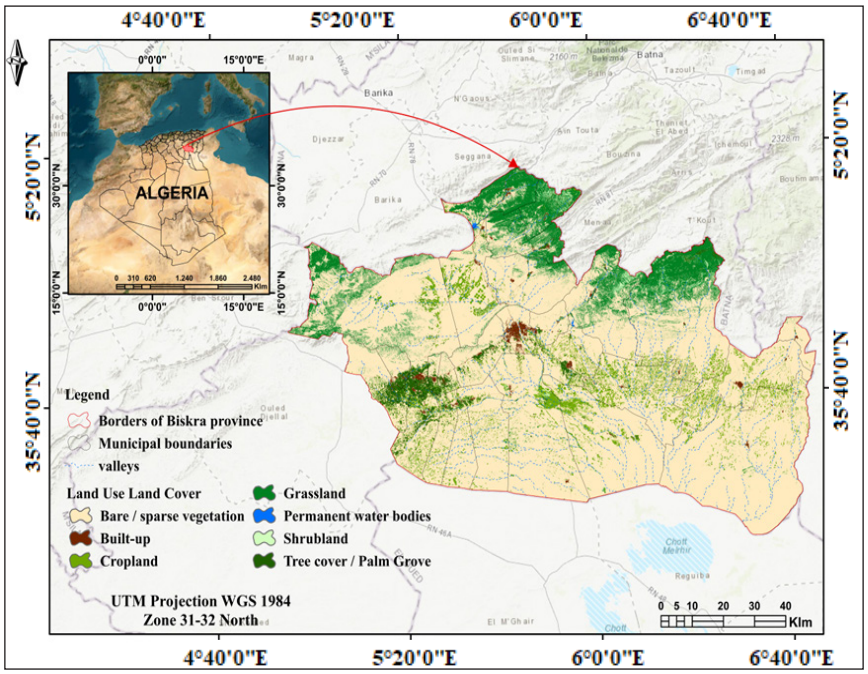


Fig. 1. Geographical location of the study area Biskra Province.

influences vegetation distribution, land use, and hydrological dynamics, making Biskra a typical example of the fragile arid ecosystems of the northern Sahara.

Floristic Composition

Due to its climatic conditions, the region is characterized by scarce precipitation and very high temperatures (Ozenda, 2004). This climatic and geomorphological variability supports a diverse but xerophytic flora well adapted to drought, salinity, and temperature extremes (Quézel and Santa, 1962). The regional flora comprises more than 400 vascular plant species, primarily from the families Poaceae, Asteraceae, Chenopodiaceae, and Fabaceae (Quézel and Santa, 1962; Ozenda, 2004; Salemkour *et al.,* 2012; Deghiche-Diab and Deghiche, 2016). Steppe vegetation is dominated by *Artemisia herba-alba*, *Stipa tenacissima*, and *Lygeum spartum*, while halophytic species such as *Atriplex halimus* and *Salsola vermiculata* prevail in saline depressions and sebkhas surrounding Chott Melghir. Psammophilous Saharan taxa, notably *Retama raetam*, *Calligonum comosum*, and *Rhanterium suaveolens* are common in sandy zones near Ourlal and *Sidi Khaled (Deghiche-Diab et al., 2016).* In the mountainous northern regions (El Kantara, M'chouneche), Mediterranean relict species like *Pinus halepensis*, *Juniperus phoenicea*, and *Rosmarinus officinalis* persist, reflecting the ecological transition from steppe to forested environments (Quézel and Santa, 1962). Human activities such as overgrazing, urban expansion, and agricultural intensification have accelerated vegetation degradation and desertification processes in the Biskra region (Tandjaoui *et al.,* 2025; Boukerker *et al.,* 2022, Deghiche-Diab, 2020).

Acquisition and Preprocessing of Satellite Data: In this study, remote sensing was conducted using Landsat satellite imagery. Specifically, Landsat 5 images were used for the year 2005, and Landsat 7 images for the years 2015 and 2025. The image acquisition periods for each year extended from January 1 to December 31 (i.e., from 01/01/2005 to 31/12/2005, from 01/01/2015 to 31/12/2015, and from 01/01/2025 to 31/12/2025, respectively), ensuring a comprehensive temporal coverage of each year. These satellites provide high-resolution data with multiple spectral bands, which is essential for a detailed analysis of vegetation dynamics. Landsat 5 offers seven spectral bands, while Landsat 7 provides eight, both with a spatial resolution of approximately 30 meters, making them suitable for monitoring vegetation and land cover change over multidecadal periods (Gorelick *et al.,* 2017; Liang *et al.,* 2023). This long-time span allows for an in-depth analysis of long-term vegetation trends in the studied region. The satellite images were downloaded from Google Earth Engine, a platform that provides easy access to a vast collection of freely available satellite data and high-performance geospatial computing (Xie *et al.,* 2019). The use of these high-resolution images enables the detection and quantification of subtle vegetation variations over time.

Vegetation Index Analysis- Normalized Difference Vegetation Index (NDVI):

The Normalized Difference Vegetation Index (NDVI) is a key indicator of vegetation health, based on the ratio between the near-infrared (NIR) and red reflectance. It is calculated using the following equation:

$$NDVI = \frac{(NIR - Red)}{(NIR + Red)} \quad ...(1)$$

where: NIR represents the near-infrared band; Red represents the red band of Landsat; NDVI values range from -1 to +1, with higher positive values indicating denser and healthier vegetation (Fayech and Tarhouni, 2021).

Soil-Adjusted Vegetation Index (SAVI)

The Soil-Adjusted Vegetation Index (SAVI) is designed to improve the accuracy of vegetation cover measurements by minimizing the influence of soil brightness. Unlike NDVI, SAVI introduces an "adjustment factor" (L) to correct for soil effects, particularly in areas with low vegetation cover. SAVI values range from -1 to +1, with higher positive values indicating denser and healthier vegetation. It is calculated using the following equation:

$$SAVI = \frac{(NIR - Red)}{(NIR + Red + L)} \times (1 + L) \quad ...(2)$$

where, NIR represents the near-infrared band; Red represents the red band; and L is the soil brightness adjustment factor.

The soil brightness adjustment factor L is an empirical parameter introduced to reduce the influence of soil reflectance in areas with sparse vegetation cover. In environments with low

vegetation density, exposed soil contributes significantly to the spectral signal, which can distort vegetation indices like NDVI (Rondeaux *et al*., 1996; Xue and Su, 2017). SAVI corrects for this by introducing L into the equation. The value of L depends on vegetation density:

L ≈ 0 for dense vegetation L ≈ 1 for bare soil

L = 0.5 is commonly used as a standard value for intermediate vegetation cover (Huete, 1988).

Enhanced Vegetation Index (EVI): The Enhanced Vegetation Index (EVI) was developed to increase the sensitivity of remote sensing to vegetation conditions, particularly in areas with dense vegetation. EVI is more responsive to variations in vegetation biomass compared to NDVI, and it addresses some of the issues related to atmospheric reflectance and soil influence. The value of EVI ranges from 0 to 1, with higher values close to 1 indicating denser and healthier vegetation. It is calculated using the following equation:

$$EVI = G \times \frac{(NIR - RED)}{(NIR + C1 \times RED - C2 \times BLUE + L)} \quad ...(3)$$

where, NIR represents the near-infrared band; Red represents the red band; Blue represents the blue band; G is a gain factor, set at 2.5; C1 and C2 are coefficients to correct atmospheric influences, set at 6 and 7.5 respectively; L is a soil adjustment factor, set at 1. (Bento *et al*., 2018; Mushtaq and Asima, 2016).

Modified Soil Adjusted Vegetation Index (MSAVI)

The Modified Soil Adjusted Vegetation Index (MSAVI) was developed to minimize the effect of soil background reflectance in areas with sparse vegetation cover. It improves upon the Soil Adjusted Vegetation Index (SAVI) by automatically optimizing the soil adjustment factor, thereby enhancing vegetation signal detection in semi-arid and arid environments. MSAVI values range from −1 to +1, where higher values indicate denser vegetation. The MSAVI is calculated using the following equation:

$$MSAVI = \frac{2 \times NIR + 1 - \sqrt{(2 \times NIR + 1)^2 - 8 \times (NIR - Red)}}{2} \quad ...(4)$$

where: NIR is the near-infrared band; Red is the red band

This index is particularly useful for vegetation monitoring in regions with exposed soils and low vegetation density (Qi *et al*., 1994).

Transformed Soil Adjusted Vegetation Index (TSAVI): The Transformed Soil Adjusted Vegetation Index (TSAVI) further reduces the soil brightness influence on vegetation signal by incorporating soil line parameters (slope and intercept). It provides a more accurate estimation of vegetation cover in heterogeneous landscapes, especially in semi-arid regions. The TSAVI is calculated using the following equation:

$$TSAVI = \frac{s \times (NIR - s \times RED - \alpha)}{(RED + s \times NIR - s \times \alpha + 0.08) \times (1 + s^2)} \quad ...(5)$$

where: NIR is the near-infrared band; Red is the red band; s is the slope of the soil line and; a is the intercept of the soil line.

TSAVI effectively corrects for soil background effects and enhances vegetation discrimination in dry and mixed land cover environments (Baret and Guyot, 1991).

Green Chlorophyll Index (GCI): The Green Chlorophyll Index (GCI) is designed to estimate chlorophyll content in vegetation canopies, which is a key indicator of plant photosynthetic activity and health status. It uses the ratio of near-infrared to green reflectance to assess chlorophyll concentration. The GCI is calculated as follows:

$$GCI = \frac{NIR}{Green} - 1 \quad ...(6)$$

where: NIR is the near-infrared band Green is the green band.

Higher GCI values indicate greater chlorophyll content, making this index valuable for assessing crop vigor and vegetation productivity (Gitelson *et al.,* 1996).

Statistical Analysis of Vegetation Indices

The analysis of vegetation indices was conducted using Python, employing the libraries Matplotlib, Seaborn, and Pandas to process and visualize the data. The main objective was to explore the relationships between different vegetation indices: NDVI, SAVI, MSAVI, TSAVI, GCI, EVI. To exanimate the correlation between variables, Pearson's correlation coefficient was used. This coefficient ranges from -1 to 1 (Benoumeldj *et al.,* 2023). An ANOVA (Analysis of Variance) test was performed to assess significant differences

between multiple groups of data based on the vegetation indices (Blanca *et al.*, 2018; Kim, 2015). To refine this analysis and specifically identify which groups stand out, a Tukey HSD post-hoc test was conducted to determine which years exhibit significant differences for each index (Ruxton and Beauchamp, 2008).

Acquisition and Preprocessing of Climatic Data: The climatic data necessary for this study, including annual average temperature and annual total precipitation, were derived from the Google Earth Engine (GEE) platform, utilizing two primary satellite/climate model datasets for the Biskra Province over the 2005, 2015, and 2025 observation periods.

These datasets were spatially and temporally aggregated within GEE to produce the annual total precipitation and annual mean temperature for the specified years, allowing for the analysis of climatic variability and its correlation with observed vegetation dynamics in Biskra Province.

Results and Discussion

Spatio-temporal analysis of vegetation dynamics using NDVI, SAVI, MSAVI, TSAVI, GCI and EVI indices for a period from 2005-2025: The obtained results for 2005, as illustrated in (Fig. 2) reveals an uneven distribution of vegetation, with dense coverage primarily concentrated in the central and northern zones, while the southeastern part shows low values, indicating areas subject to significant ecological stress. Values ranged from -0.43 to 0.60, reflecting moderately dense vegetation but also the presence of degraded areas. By 2015, a clear improvement is observed, with maximum values reaching 0.75. This progression indicates a relative recovery of vegetation cover, particularly in the central and northeastern sectors, although degraded areas persist in the southeast, reflecting ongoing environmental challenges. In 2025, a slight decline in maximum NDVI values was observed, reaching approximately 0.69, alongside an expansion of areas with sparse vegetation. This moderate decrease suggests a progressive degradation of vegetation in some locations, although dense vegetation areas persist, revealing a degree of ecological resilience face to environmental pressures. These trends are comparable to the NDVI developments observed between 2000 and 2020, the vegetation initially shows improvement, followed by stabilization, or even slight degradation, with the persistence of core areas of high-density vegetation that testify to an enduring ecological resistance.

The SAVI maps (Fig. 3) illustrate the consistent spatial pattern of vegetation density in the Biskra region, characterized by a fundamental dichotomy between small pockets of high density and widespread bareness. The SAVI 2005 map establishes the baseline, showing peak vegetation density to be highly localized in the northern and north-western parts of the study area, reaching a maximum value of 0.6615. Crucially, the majority of the map is covered by less values, signifying low SAVI values and therefore sparse vegetation or exposed soil across the vast regional landscape. The SAVI 2015 map indicates a slight decline in peak density, with the maximum value dropping to 0.6109. The areas of high density remain similarly restricted, but the overall shift suggests a regional lowering of SAVI values compared to the baseline. This drop in peak density, combined with the observed sharp collapse in GCI and EVI during the same period, confirms that the region's vegetation was undergoing significant stress between 2005 and 2015. The SAVI 2025 map shows a visually consistent spatial distribution: localized high-density areas persist, but they are isolated.

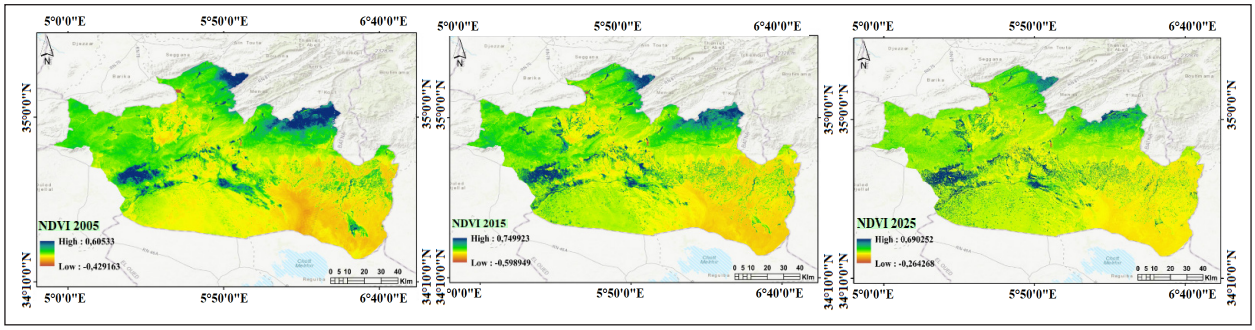


Fig. 2. Normalized Difference Vegetation Index (2005-2015-2025).

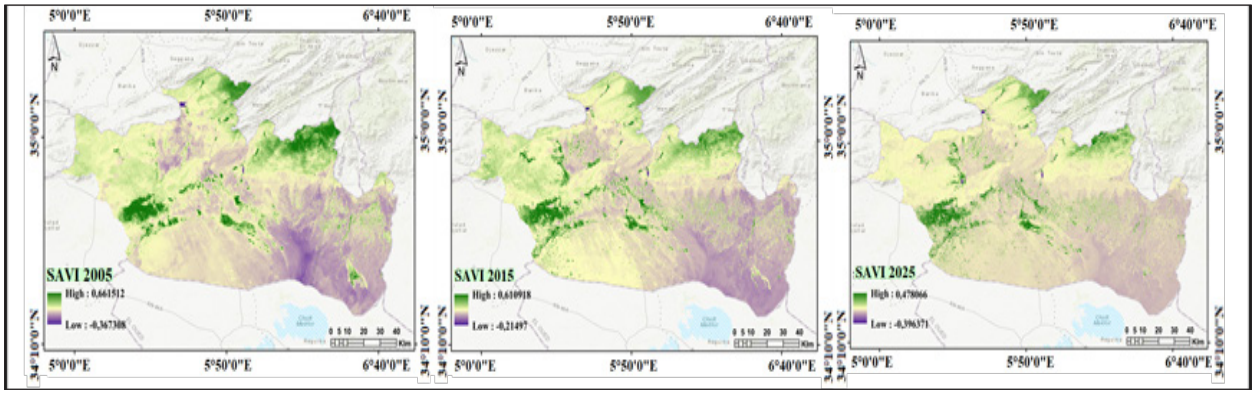


Fig. 3. Soil Adjusted Vegetation Index (2005-2025).

However, the maximum value reaches a high of 1.000, which, if accurate, suggests extremely high localized density (perhaps due to intensive irrigation). The region shows widespread low vegetation cover and degradation, with sparse vegetation prevailing despite localized higher values.

The 2005 EVI map (Fig. 4) shows a heterogeneous vegetation distribution across the study area. Areas with the highest EVI values, reaching up to 0.57, are located mainly in the north and northwest regions, indicating denser and healthier vegetation cover. The central and southern parts display predominantly lower EVI values, with large yellow and orange regions, suggesting sparse or degraded vegetation. This pattern reflects the impact of climatic and anthropogenic pressures, with only limited zones supporting dense vegetation cover. By 2015, there was a noticeable improvement in vegetation cover as illustrated by increased EVI values, which reach a maximum of approximately 0.59. Dense green areas expand further, particularly in the northern and central parts of the region, indicating either successful land management or favorable climatic conditions over the decade. However, yellow and orange tones persist in the southern and southeastern areas, highlighting that while some recovery has occurred, extensive regions still endure ecological stress and Low vegetation cover. The 2025 EVI map demonstrates a slight shift in vegetation dynamics compared to previous years. Maximum EVI values rise to approximately 0.68, but the dense green zones remain restricted mostly to the north and northwest. Much of the territory is still covered in yellow, indicating moderate to low vegetation activity. This suggests that despite some resilience and localized improvement, large tracts of the area continue to experience challenges in maintaining dense vegetation, possibly due to persistent environmental stressors or land use changes. Overall, the series of maps shows gradual but limited improvement in vegetation cover over two decades, with northern regions consistently exhibiting greater ecological vitality than the drier southern areas.

The MSAVI index (Fig. 5) in 2005 recorded a maximum value of 0.623415, while the minimum value dropped to -0.455202. Vegetation distribution showed a notable concentration in the northwestern regions and some parts of the northeast. However, the central, eastern,

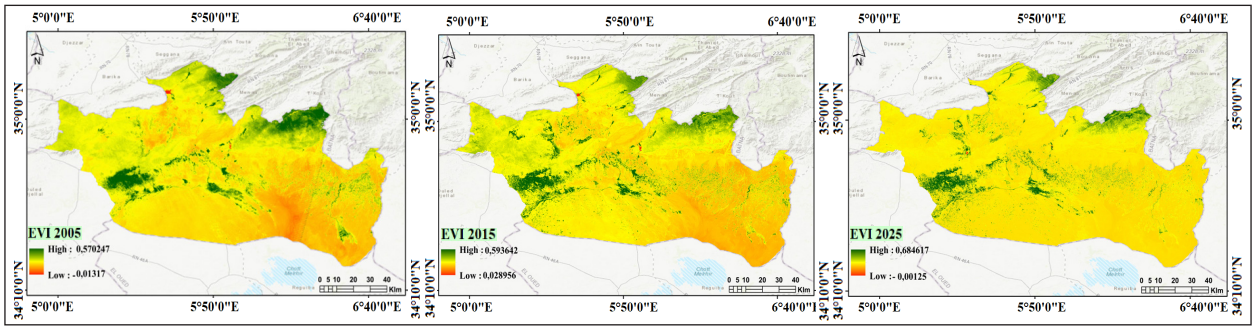


Fig. 4. Enhanced Vegetation Index (2005-2025).

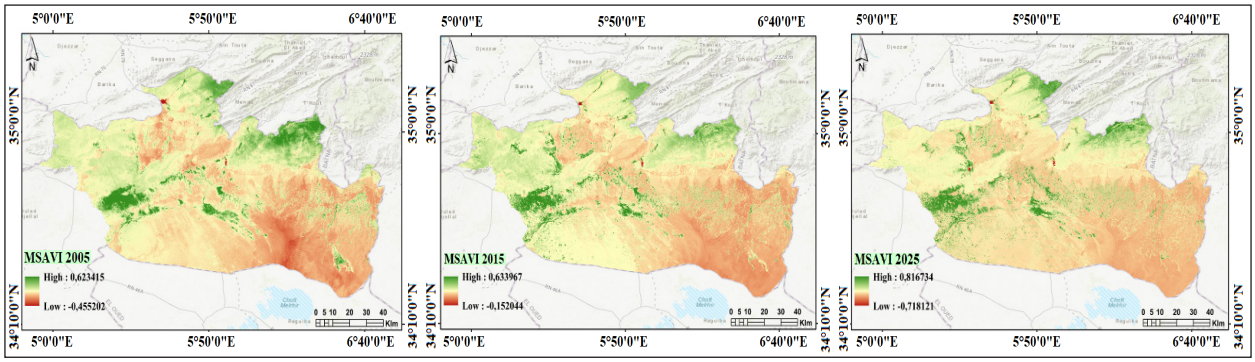


Fig. 5. Modified Soil Adjusted Vegetation Index (2005-2025).

and southern areas recorded low values, indicating the dominance of Low vegetation cover or significant soil influence across most of the region. In 2015, the maximum index value slightly increased to 0.633967, while the minimum value improved compared to 2005, reaching -0.152044. A minor improvement in the health and density of vegetation was observed in areas with peak values, yet the spatial distribution of dense vegetation remained confined to the same northern and western zones. The central and southeastern areas continued to display values reflecting clear environmental variability, indicating persistent challenges related to scarce vegetation and soil influence. The 2025 data show a significant leap in the maximum MSAVI value, which has reached 0.816734, while the minimum value has dropped to -0.718121. This high maximum value reflects a notable improvement in the density and health of vegetation in the highest-value areas, indicating an extremely healthy vegetation condition. However, the general spatial pattern remains similar to previous years: dense vegetation is concentrated in the northwestern and northeastern regions, while other areas continue to suffer from low MSAVI values, confirming the persistence of environmental degradation challenges and bare soil across vast expanses. From 2005 to 2015, Stability with a slight improvement in the health of peak vegetation (from 0.62 to 0.63). From 2015 to 2025, A significant projected improvement in the highest-density vegetation areas, with the index jumping to approximately 0.81. Despite the improvement in maximum values, the spatial distribution of dense vegetation remains limited to specific areas, while low values prevail in the central, eastern, and southern regions, indicating the dominance of environmental challenges such as drought and soil quality across most of the region.

The TSAVI index (Fig. 6), which measures vegetation density while minimizing soil brightness effects, reveals a distinct degradation and partial recovery pattern in the peak vegetation density across the Biskra region, alongside persistent spatial heterogeneity. The TSAVI 2005 map established a high baseline for peak vegetation density, with a maximum value of 0.943475. This near-unity value signifies a high capability for dense vegetation cover in localized areas. The minimum value was 0.407268, highlighting data inconsistency, but the focus remains on the peak decline). By 2015, the maximum TSAVI value suffered a significant decline to 0.610214. This drop of approximately 35% from the 2005 peak indicates a substantial loss of the highest density vegetation cover during this decade.

This degradation is consistent with the general ecological stress evident across other indices (like the GCI collapse from earlier data) and is likely a result of the warming climate and unreliable precipitation. The minimum value shifted to 0.469543. By 2025 TSAVI illustrates a moderate level of vegetation recovery compared with previous years. The maximum value reached 0.943475, representing a partial improvement over the 2015 peak but still remaining below the 2005 baseline. This indicates that while some areas have experienced a degree of ecological restoration, the environment has not yet regained its former vegetation density or health observed in earlier periods. The minimum value for 2025 was 0.463601, suggesting the persistence of degraded or sparsely vegetated surfaces in several parts of the region. Spatially, zones of high vegetation density were still restricted to small, localized

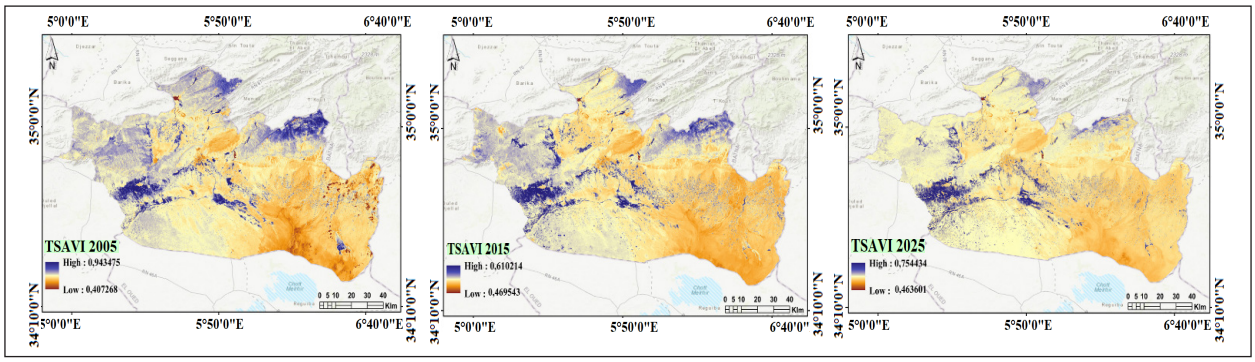


Fig. 6. Transformed Soil Adjusted Vegetation Index (2005-2025).

pockets, particularly in areas with favorable hydrological or soil conditions. The dominant values continue to reflect low vegetation cover and widespread arid conditions, emphasizing the ongoing environmental stress affecting much of Biskra Province. Overall, the 2025 TSAVI distribution reveals partial but limited ecological recovery, characterized by localized vegetation resurgence within a broader context of persistent aridity. This pattern underscores the region's fragile ecological balance and its vulnerability to both climatic variability and anthropogenic land-use pressures.

The GCI 2005 map (Fig. 7) shows a localized peak health with a maximum value of 0.99913. This value is very close to the theoretical maximum (1.0), indicating excellent localized plant health and photosynthetic activity in certain pockets. The minimum value is recorded at 0.10683. Spatially, the majority of the region shows low to moderate health, while the high values are restricted to small areas. The GCI 2015 map shows a maximum value of 0.99946. This was virtually identical to the 2005 peak, suggesting that the highest localized plant health remained stable during this period, the minimum value increased slightly to 0.18523. Visually, the map maintains the pattern of localized high health surrounded by vast areas of low to moderate health. The 2025 GCI map reveals maintained stability in maximum chlorophyll values recording 0.99823, which indicates preserved peak health conditions in the most vigorous vegetation areas at near-theoretical maximum levels. However, the observed minimum value has decreased to 0.05074, highlighting continued stress in vulnerable zones. Spatially, the data confirms that high-health vegetation remains restricted to small, isolated pockets, while the majority of the landscape continues to experience significant health challenges. In summary, while maximum GCI values demonstrate remarkable stability approaching 1.0 throughout the 2005-2025 period, the persistent spatial concentration of these high values confirms that successful vegetation growth remains limited to specific, localized areas, rather than indicating broad regional improvement in plant health across the study area.

Analysis of Vegetation Indices Trends and Boxplots (2005-2025): The Fig. 8 track the median values of six vegetation indices (NDVI, SAVI, MSAVI, TSAVI, EVI, and GCI) in the Biskra region from 2005 to 2025. The results reveal two distinct phases of vegetation dynamics,

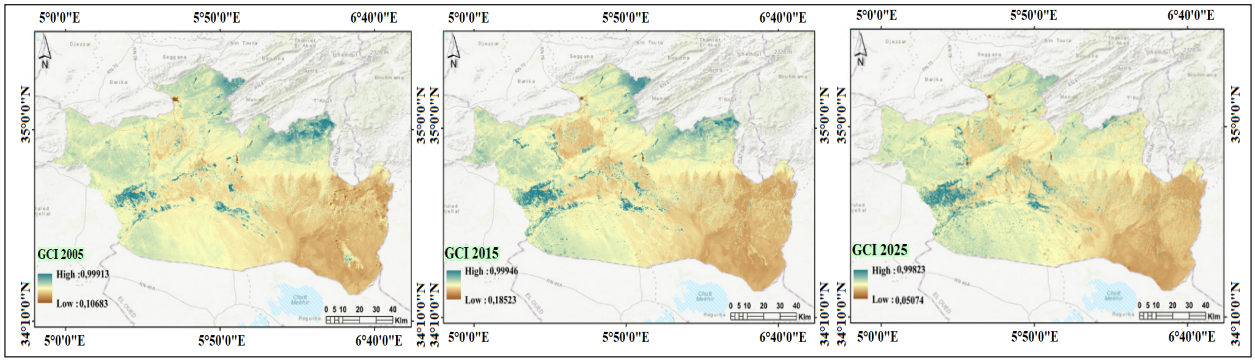


Fig. 7. Green Chlorophyll Index (2005-2025).

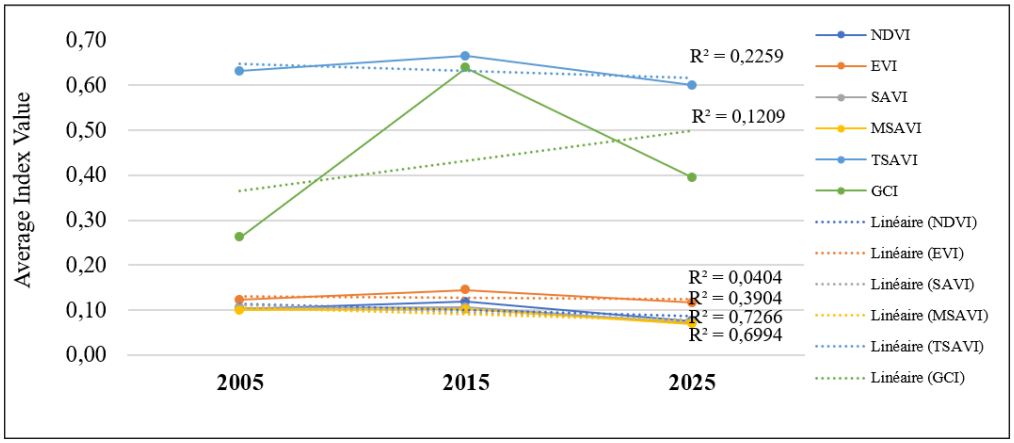


Fig. 8. Average Vegetation Indices Over Years (2005-2025).

it reveals a clear and concerning trend of ecological degradation. While conditions remained relatively stable between 2005 and 2015, the subsequent decade witnessed a marked decline across nearly all indices. The Enhanced Vegetation Index (EVI) dropped from 0.122 to 0.071, indicating a significant reduction in canopy density and structure. Similarly, the NDVI decreased from 0.103 to 0.076, reflecting an overall deterioration in green vegetation cover. Whereas the most alarmingly, the Modified Soil-Adjusted Vegetation Index (MSAVI) plummeted from 0.105 to just 0.010, suggesting dramatically increased soil exposure and reduced vegetation density. This consistent downward trajectory across multiple indices underscores the escalating environmental stress in this arid region. The analysis indicates marked vegetation degradation between 2005 and 2015, followed by stabilization at low levels after 2015. Most of the Biskra region exhibits poor vegetation cover, with healthy vegetation restricted to limited northern areas.

The statistical distribution of vegetation indices, as illustrated through boxplots (Fig. 9), reveals significant shifts in the region's ecological health over two decades. The analysis differentiates between low-value indices (NDVI, MSAVI, SAVI, EVI) and higher-value indices (TSAVI, GCI), both demonstrating a notable transition from relative stability to marked deterioration. For the low-value indices, the initial period (2005–2015) showed a slight improvement, with minor increases in median values and interquartile ranges (IQR). However, the subsequent decade (2015–2025) witnessed a clear reversal, characterized by declining medians and narrowing IQRs. This trend indicates not only a reduction in vegetation density and health but also a homogenization of conditions toward lower values across the region. Similarly, the higher-value indices, TSAVI and GCI, mirrored this pattern, with an initial period of stability followed by a significant decline in both median and IQR values. This parallel deterioration confirms

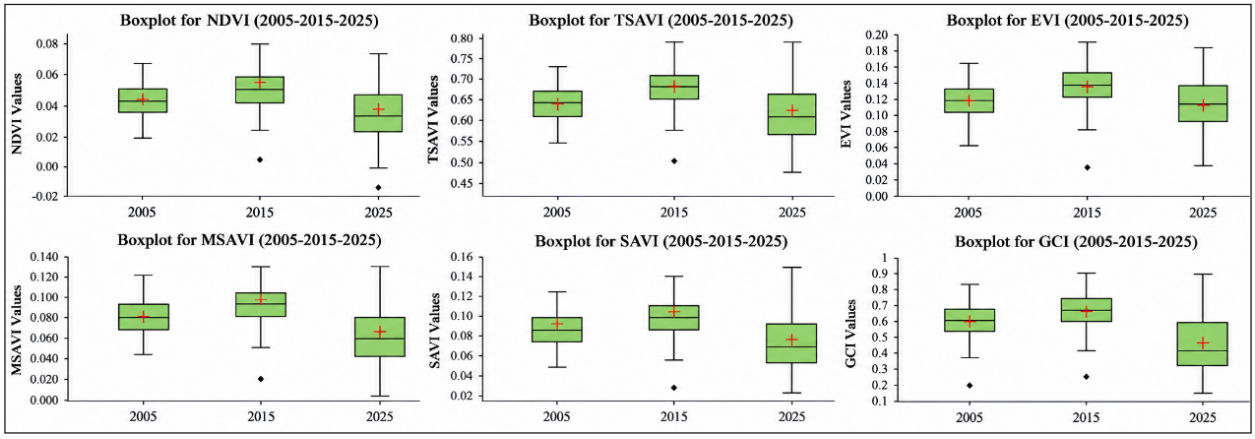


Fig. 9. Boxplot for Indices Average (2005-2025).

that the ecological decline affected not only vegetation density but also plant health and soil-adjusted vegetation characteristics. This statistical evidence underscores a pervasive ecological challenge, overriding any localized improvements and emphasizing the need for targeted interventions to address the widespread decline in vegetation health and coverage.

Correlation between Vegetation Indices: As represented in Figure10 that shows the correlation between the indices. This correlation matrix highlights the relationships between three vegetation indices: EVI, NDVI, GCI, MSAVI, TSAVI and SAVI.

The correlation matrix presents Pearson's coefficients (r) among six vegetation indices (EVI, SAVI, NDVI, MSAVI, TSAVI, and GCI) for 2005, 2015, and 2025. Across all three years, NDVI, EVI, SAVI, MSAVI, and TSAVI show very strong positive correlations, with r consistently > 0.90 and frequently > 0.99 (NDVI–MSAVI = 0.9939 in 2005). This reflects their shared dependence on high NIR reflectance and red-band absorption by vegetation. Despite soil-adjustment corrections in SAVI, MSAVI, and TSAVI, these indices respond similarly to vegetation biomass and canopy structure, explaining their near-redundant behavior.

GCI exhibits a distinct correlation pattern relative to the other indices, especially in 2015 and 2025. In 2005, GCI shows strong positive correlations with the other indices (≈0.90-0.97), notably with EVI (r = 0.9704) and SAVI (r = 0.9705), indicating a comparable response to vegetation conditions, though slightly weaker. However, in 2015 and 2025 these relationships weaken markedly, becoming low or near-zero. By 2025, correlations are very weak with EVI (r = 0.2033), SAVI (r = 0.2041), and NDVI (r = 0.2433), highlighting a decoupling of chlorophyll-related signals from structural vegetation indices under increased environmental stress.

The GCI uses the Green band, which is more sensitive to chlorophyll content (and often less affected by high LAI saturation than NDVI). The decreasing correlation over time suggests that, in later years (2015 and 2025), the changes in chlorophyll content (GCI) are decoupling from the changes in biomass/structure (NDVI, EVI, etc.). This could indicate:

- *vegetation stress/senescence*: The plants are losing chlorophyll (decrease in GCI) while maintaining high structural density (still high

Year 2005	EVI	SAVI	NDVI	MSAVI	TSAVI	GCI
EVI	1	0,996	0,990	0,995	0,995	0,970
SAVI	0,996	1	0,997	1,000	0,996	0,974
NDVI	0,990	0,997	1	0,997	0,987	0,962
MSAVI	0,995	1,000	0,997	1	0,994	0,977
TSAVI	0,995	0,996	0,987	0,994	1	0,977
GCI	0,970	0,974	0,962	0,977	0,977	1

Year 2015	EVI	SAVI	NDVI	MSAVI	TSAVI	GCI
EVI	1	0,983	0,971	0,976	0,909	0,672
SAVI	0,983	1	0,974	0,997	0,919	0,787
NDVI	0,971	0,974	1	0,953	0,838	0,725
MSAVI	0,976	0,997	0,953	1	0,942	0,801
TSAVI	0,909	0,919	0,838	0,942	1	0,759
GCI	0,672	0,787	0,725	0,801	0,759	1

Year 2025	EVI	SAVI	NDVI	MSAVI	TSAVI	GCI
EVI	1	0,986	0,980	0,980	0,932	0,704
SAVI	0,986	1	0,981	0,998	0,941	0,804
NDVI	0,980	0,981	1	0,965	0,883	0,743
MSAVI	0,980	0,998	0,965	1	0,957	0,819
TSAVI	0,932	0,941	0,883	0,957	1	0,789
GCI	0,704	0,804	0,743	0,819	0,789	1

Fig. 10. Correlation Matrix of Vegetation Indices (EVI, SAVI, NDVI, GCI, MSAVI, TSAVI).

Table 1. One-Way ANOVA Results

Index	F-statistic	P-value	Significance (α=0.05)
NDVI	745.58	8.50×10^{-309}	Significant
EVI	344.51	7.27×10^{-147}	Significant
SAVI	764.32	3.67×10^{-316}	Significant
MSAVI	730.30	8.90×10^{-303}	Significant
TSAVI	996.90	$<1.0\times10^{-322}$	Significant
GCI	3627.12	$<1.0\times10^{-322}$	Significant

NDVI/EVI), which often precedes a decline in vigor.

- *changing vegetation type*: A shift to a type of vegetation where the relationship between canopy greenness and canopy structure is less direct.

Analysis of Temporal Variations in Vegetation Indices Using ANOVA and Tukey's Post-Hoc Test: The analysis of temporal variations in the six vegetation indices (NDVI, EVI, SAVI, MSAVI, TSAVI, and GCI) was conducted using a One-Way Analysis of Variance ANOVA for 2005, 2015, 2025 (Table 1). The ANOVA results indicated a highly statistically significant effect of time on the mean values of all six vegetation indices (P = 0.001), confirming that substantial differences exist in vegetation conditions across the studied years. The F-statistics were universally high (e.g., GCI at F 3627.12), demonstrating that the temporal grouping accounts for a massive proportion of the total variance in the data for every index. All six vegetation indices showed a highly significant difference in mean values (P < 0.05) across 2005, 2015, and 2025.

The comprehensive temporal analysis, integrating ANOVA, Tukey's HSD post-hoc testing, and box plot (Fig.11) visualizations across the six vegetation indices (NDVI, EVI, SAVI, MSAVI, TSAVI, and GCI), The analysis clearly shows significant changes in vegetation from 2005 to 2025. A two-phase pattern emerges: improvement peaking around 2015, followed by a sharp, statistically significant decline by 2025. Chlorophyll-sensitive indices (GCI)

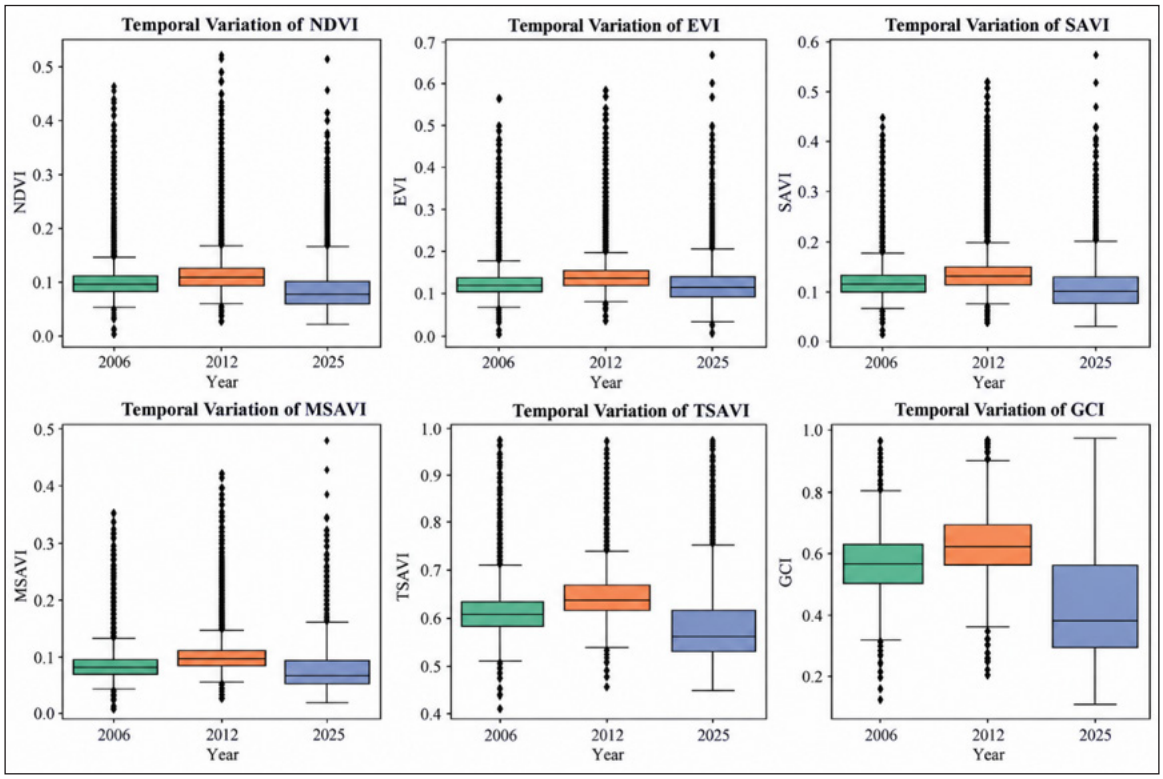


Fig. 11. Analysis of Temporal Variations in Vegetation Indices Using ANOVA and Tukey's Post-Hoc Test.

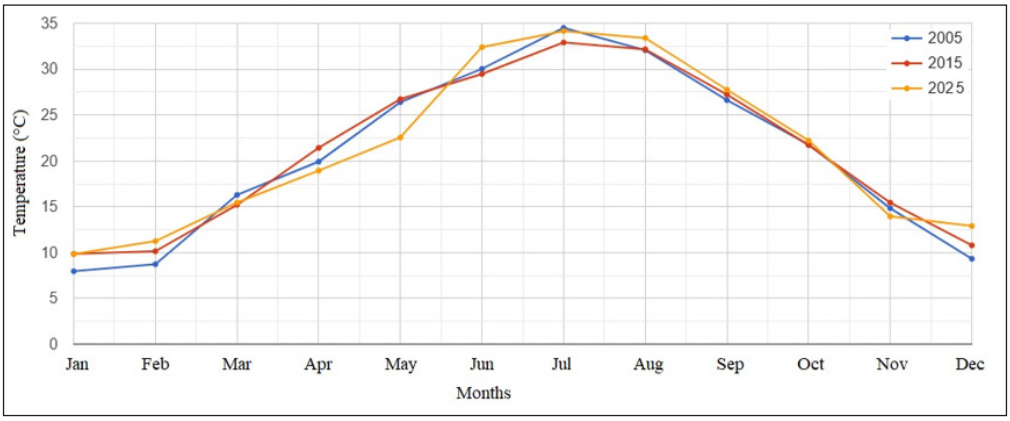


Fig. 12. Variation in Temperature (2005-2025).

showed the greatest loss, alongside increased spatial variability, indicating localized stressors drove widespread degradation.

Variation in Precipitation and Temperature (Comparative Analysis between 2005, 2015, and 2025): Temperature data from 2005-2025 (Fig. 14) show a clear warming trend in Biskra's hot arid climate. Winter averages rose from 8-9°C in 2005 to ~10°C in 2015, with modest shoulder-season increases. By 2025, May was 3°C warmer than 2005, and July peaks reached 35°C. Warming was most pronounced in spring and autumn, altering the seasonal thermal profile.

Rising temperatures strongly correlate with vegetation degradation (Fig. 12). Warming during critical growth months (May-July) increased evapotranspiration and water stress, reflected in declining NDVI, EVI, and GCI values (2015-2025). Accelerated spring warming and prolonged autumn heat shortened the optimal growing period. Temperature extremes, affecting both minima and maxima, are a key driver of widespread ecological decline, outweighing localized vegetation gains and intensifying Biskra's environmental challenges.

Combining vegetation indices with climate data reveals clear environmental stress in the Biskra region. The precipitation data for the Biskra region (Fig. 13) reveals significant changes in rainfall patterns over the two-decade period from 2005 to 2025. In 2005, conditions were most favorable, with higher spring and autumn rainfall supplying sufficient moisture for plant growth. By 2015, rainfall declined, especially in winter, though an extreme 35 mm event in October reflected rising climate variability. 2025 data confirm continued drying, with minimal winter and spring rainfall severely limiting water for vegetation during key growth periods. The integration of vegetation indices

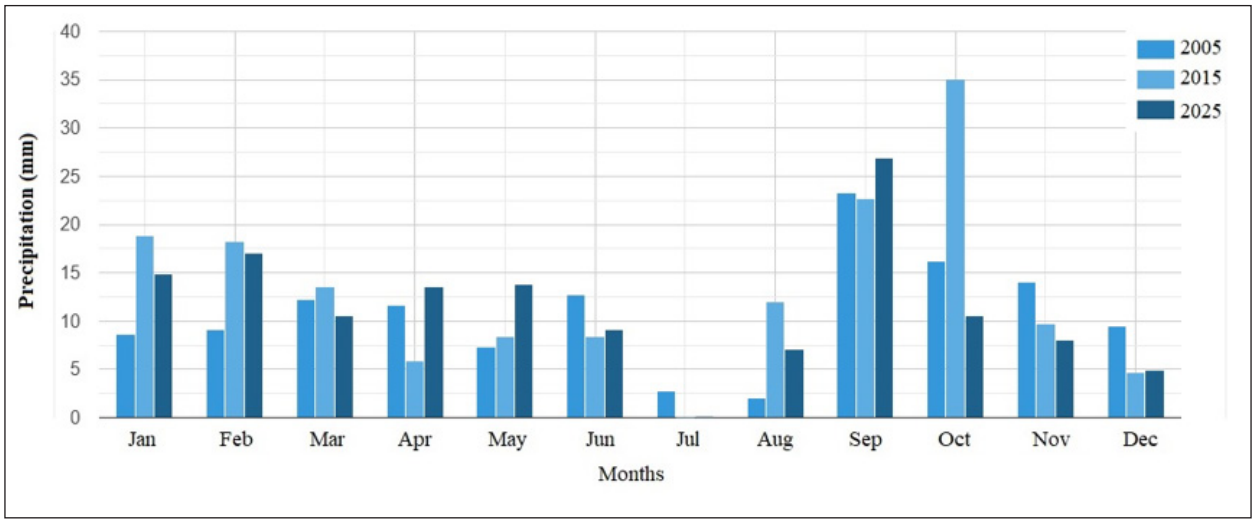


Fig. 13. Variation in precipitation (2005-2025).

with climate data presents a coherent picture of environmental stress in the Biskra region. Rising temperatures, especially in transitional seasons, have increased evapotranspiration and plant water stress. Combined with declining and more erratic rainfall through 2025, these conditions have severely limited water availability, directly driving the sharp decline in vegetation indices between 2015 and 2025, with median values stabilizing at low levels across the region.

The Biskra region, located in southeastern Algeria, presents a compelling case study of profound ecological transformation in an arid environment, is a striking example of the complexity of ecological dynamics where the interactions between biotic, abiotic, and anthropogenic factors lead to an accelerated degradation of ecosystem. The analysis of median values for six vegetation indices (NDVI, SAVI, MSAVI, TSAVI, EVI, GCI) from 2005 to 2025 reveals two distinct phases of vegetation dynamics, highlighting an initial phase of pronounced degradation followed by a fragile stabilization.

Vegetation indices for Biskra in 2005, 2015, and 2025 reveal complex ecological dynamics, showing overall degradation in vegetation quality and density, especially in the semi-arid and desert southern and central areas. Northern regions remained relatively stable or variable. Correlation analysis underscores the complementarity of indices, highlighting the value of a multi-index approach for accurately assessing vegetation interactions with soil and climate (Catry *et al.,* 2012a; Alves *et al.,* 2010).

NDVI, shows relative spatial stability, with high values concentrated in the north and low values in the central and southern regions. Over 2005–2025, high-density areas have slightly declined, particularly at the edges of dense vegetation, suggesting desertification or localized degradation. The moderate negative correlation with EVI (–0.69) arises because NDVI saturates in high-biomass areas, limiting its ability to detect subtle differences in vegetation density (Deghiche-Diab, 2019; Zou *et al.,* 2022; Rahimi and Dong, 2025; Mersha *et al.,* 2024).

The SAVI, MSAVI, and TSAVI indices, which account for soil reflectance, underscore the significant influence of soil conditions on vegetation in Biskra province. The predominance of low SAVI/MSAVI and TSAVI values in the southern and central regions confirms the prevalence of sparse vegetation and the strong impact of bare soil, indicative of ongoing desertification. Notably, the 2025 SAVI data reveal a marked reduction in vegetated areas compared to 2005 and 2015, reflecting widespread degradation in sensitive zones. Because SAVI explicitly incorporates soil effects into its calculation, it is particularly effective for detecting vegetation stress in areas where soil conditions strongly affect plant growth (Baret and Guyot, 1991; Rahimi and Dong, 2025). These results highlight the critical role of soil–vegetation interactions in shaping ecosystem vulnerability and the importance of incorporating soil-adjusted indices in ecological monitoring of arid and semi-arid landscapes.

GCI shows high values confined to the north, while low values dominate most of the province, indicating generally low chlorophyll content and vegetation vigor across the region. The correlation matrix highlights a key trend: the increasing divergence of the Green Chlorophyll Index (GCI) from the other vegetation indices over the 20-year period. In 2005, all indices exhibit strong positive inter-correlations, reflecting uniform vegetation growth where biomass and chlorophyll content are closely coupled (Huete, 1988; Baret and Guyot, 1991). By 2015 and especially 2025, the structural indices (NDVI, EVI, SAVI, MSAVI, TSAVI) remain highly correlated with each other, but their association with GCI declines sharply. By 2025, correlations are very weak, indicating that GCI is capturing a decoupled aspect of vegetation, likely related to plant health, senescence, or chlorophyll reduction, which the structural indices no longer fully reflect. This underscores the importance of including chlorophyll-sensitive indices like GCI to assess vegetation condition under increasing environmental stress (Zou *et al.,* 2022; Rahimi *et al.,* 2025).

From 2005 to 2015, median vegetation health declined sharply, especially in GCI and EVI, reflecting major losses in chlorophyll content and canopy structure, while NDVI, SAVI, and MSAVI remained consistently low, indicating sparse vegetation dominated by soil background. The stability of TSAVI suggests its sensitivity to arid soil conditions rather than vegetation vigor (Baret and Guyot, 1991; Huete, 1988). After 2015,

no recovery was observed; instead, all indices converged and stabilized at critically low levels, indicating a degraded ecological equilibrium. This two-phase dynamic is consistent with the combined effects of anthropogenic pressure, rising temperatures, and prolonged drought, which intensify evapotranspiration and soil aridity and drive vegetation collapse in arid environments (Boukerker *et al.,* 2022; Wu *et al.,* 2024; Abbas, 2024).

The discrepancies between the different indices suggest that degradation in Biskra Province may not only be a loss of green area, but also a change in vegetation quality and degradation of soil characteristics. The decline in EVI and SAVI in parallel with stability or slight decline in NDVI can be explained by a combination of factors, including; climatic stress, characterized by rising temperatures and reduced rainfall, leads to a decline in plant vigor (lower EVI) and increased soil reflectance due to drought (lower SAVI/ MSAVI) (De la Cruz *et al.,* 2014; Catry *et al.,* 2017). The reduction in summer precipitation directly affects plant survival by increasing water stress, thereby making the ecosystem more vulnerable to drought (Chouiter *et al.,* 2024). Such conditions drastically increase evapotranspiration, exacerbate soil dryness, and reduce the water use efficiency of plants, particularly during the growing season (Barbati *et al.,* 2012; Catry *et al.,* 2012b; Boucif *et al.,* 2024). Higher temperatures can also accelerate plant senescence and increase the risk of forest fires (Bouget *et al.,* 2023; Moreira *et al.,* 2009).

The observed declines in vegetation quality and density could potentially be attributed to biological stressors, particularly pest species such *as Lymantria dispar* and *Tortrix viridana*, which are known to adversely affect plant health and growth (DGF, 2020; Aouissi *et al.,* 2021; Abbas, 2024) which cause massive defoliation (Tiberi *et al.,* 2016; Gidey *et al.,* 2018), or may be attribute to the pathogenic fungi *Biscogniauxia mediterranea* (**Sanchez-González** *et al.,* 2010; Nadezhdina *et al.,* 2008), that may also contribute to degradation.

Anthropogenic pressures, including intensive deforestation for agriculture, urban expansion, overgrazing (Chouiter *et al.,* 2024), and humancaused forest fires, contribute to increased habitat fragmentation and a reduction in forested areas. In addition, large wildfires have directly destroyed vegetation cover, degraded soils, and disrupted ecosystem structure and function, further exacerbating habitat loss and weakening ecosystem resilience in vulnerable dryland landscapes (Curt *et al.,* 2020; Abbas, 2024).

Conclusion

The 2015–2025 period marks a critical phase of accelerated degradation, indicating that much of the Biskra region has crossed an ecological threshold. Rather than a complete collapse, the region shows strong vegetation polarization, with resilient cores surrounded by extensive degraded areas vulnerable to aridity and human pressure. This situation highlights the urgent need for spatially targeted management, emphasizing water and soil conservation, protection of remaining vegetated zones, and restoration efforts to promote broader ecological recovery.

Acknowledgements

The lead author would like to express her sincere gratitude to her colleague for the constructive feedback. She also extends her deep appreciation to the Ministry of Higher Education and Scientific Research (MESRS) and to the General Directorate for Scientific Research and Technological Development (DGRSDt) for their valuable support.

References

Abbas, S. 2024. Diachronic study of changes in vegetal cover in a mountainous ecosystem by spatial remote sensing: case of the Aures mountains (Algeria). *Technium: Romanian Journal of Applied Sciences and Technology* 24: 58-75. doi:10.47577/technium.v24i.11749

Alves, L.F., Vieira, S.A., Scaranello, M.A., Camargo, P.B., Santos, F.A.M., Joly, C.A. and Martinelli, L.A. 2010. Forest structure and live aboveground biomass variation along an elevational gradient of tropical Atlantic moist forest (Brazil). *Forest Ecology and Management* 260(5): 679-691. doi:10.1016/j.foreco.2010.05.023

Aouissi, HA., Deghiche-Diab, N. and Farhi, Y. 2021. Etat actuel de la faune Algérienne, sauvage et domestique. *Edition Universitaies Européenne* 300 p.

Bai, Z.G., Dent, D.L., Olsson, L. and Schaepman, M.E. 2008. Proxy global assessment of land degradation. *Soil Use and Management* 24(3): 223-234.

doi:10.1111/j.1475-2743.2008.00169.x

Barbati, A., Salvati, R., Ferrari, B., Di Santo, D., Quatrini, A., Portoghesi, L., Travaglini, D., Iovino, F. and Nocentini, S. 2012. Assessing and promoting old-growthness of forest stands: Lessons from research in Italy. *Plant Biosystems* 146(1): 167-174.

doi:10.1080/11263504.2011.650730

Baret, F. and Guyot, G. 1991. Potentials and limits of vegetation indices for LAI and APAR assessment. *Remote Sensing of Environment* 35(2-3): 161-173.

doi:10.1016/0034-4257(91)90009-U

Benoumeldj, M., Rached-Kanouni, M., Chouiter, N., Bouchareb, A. and Ababsa, L. 2023. Exploring the association between vegetation cover and land surface temperature in Constantine: A comparative analysis. *Revue des BioRessources* 13(2): 50-65. https://dspace.univ-Ouargla.dz/jspui/handle/123456789/35369

Bento, V.A., Gouveia, C.M., DaCamara, C.C. and Trigo, I.F. 2018. A climatological assessment of drought impact on vegetation health index. *Agricultural and Forest Meteorology* 259: 286-295.

doi:10.1016/j.agrformet.2018.05.014

Berdugo, M., Delgado-Baquerizo, M., Soliveres, S., Hernández-Clemente, R., Zhao, Y., Gaitán, J. J., Gross, N., Saiz, H., Maire, V., Lehmann, A., Rillig, M.C., Solé, R.V. and Maestre, F.T. 2020. Global ecosystem thresholds driven by aridity. *Science* 367 (6479): 787–790.

doi:10.1126/science.aay5958

Blanca, M.J., Alarcón, R., Arnau, J., Bono, R. and Bendayan, R. 2018. Effect of variance ratio on ANOVA robustness: Might 1.5 be the limit? *Behavior Research Methods* 50(3): 937-962.

doi:10.3758/s13428-017-0918-2

Boucif, O.E.W., Rached-Kanouni, M. and Chouiter, N. 2024. Phytochemical characterization and valorization of Quercus ilex (west of Algeria). *Global NEST Journal* 26(10): 06636.

doi:10.30955/gnj.06636

Bouget, C., Cours, J. and Sallé, A. 2023. Forêts en crise et biodiversité : menaces et opportunités. Effets des dépérissements et de leur gestion sur la biodiversité forestière. *Revue forestière française* 74(2): 193-199.

doi:10.20870/revforfr.2023.7594

Boukerker, H., Hecini, L., Salemkour, N., Boumedjane, M. R., Kherifi, W. and Diab, N. 2022. Impacts of grazing and restoration by planting on the pastoral potential, floristic richness and diversity of the southwestern steppe of Naâma (Algeria). *Livestock Research for Rural Development* 34(8). https://www.lrrd.cipav.org.co/lrrd34/8/3468hbou.html

Catry, F.X., Branco, M., Sousa, E., Caetano, J., Naves, P. and Nóbrega, F. 2017. Presence and dynamics of ambrosia beetles and other xylophagous insects in Mediterranean cork oak forest following fire. *Forest Ecology and Management* 404: 45-54.

doi:10.1016/j.foreco.2017.08.029

Catry, F.X., Moreira, F., Cardillo, E. and Pausas, J.G. 2012b. Post-fire management of cork oak forests. In *Post-fire Management and Restoration of Southern European Forests* (Eds. F. Moreira, M. Arianoutsou, P. Corona and J. De las Heras), *Managing Forest Ecosystems* 24: 195-222. Springer, Dordrecht.

doi:10.1007/978-94-007-2208-8_9

Catry, F.X., Moreira, F., Cardillo, E., and Pausas, J.G. 2012a. Post-fire management of cork oak forests. In: Post-fire Management and Restoration of Southern European Forests (Eds. F. Moreira, M. Arianoutsou, P. Corona and J. De las Heras), Managing Forest Ecosystems 24: 195-222. Springer, Dordrecht. Doi: 10.1007/978-94-007-2208-8_9

Chen, I.-C., Hill, J. K., Ohlemüller, R., Roy, D.B. and Thomas, C.D. 2011. Rapid range shifts of species associated with high levels of climate warming. *Science* 333(6045): 1024-1026.

doi:10.1126/science.1206432

Chouiter, N., Rached-Kanouni, M. and El Wahida Boucif, O. 2024. Assessment of the health status of oak trees in the Zouagha forest (north-east of Algeria). *Ekológia* (*Bratislava*) 43(2): 158-166.

doi:10.2478/eko-2024-0016

Curt, T. and Rigolot, E. 2020. Prévenir les risques d'incendies de forêt dans un contexte de changement global. *Sciences Eaux & Territoires* 33(3): 50-55.

doi: 10.3917/set.033.0050.

Deghiche-Diab, N. and Deghiche, L. 2016. *La flore spontanée des oasis des Ziban, Biskra-Algérie*. (Eds) Éditions universitaires européennes. 300 p.

Deghiche-Diab, N., Deghiche, L. and Kachai, S. 2016. Importance of spontaneous plants of steppe arid regions Ouled Djellel Biskra (Algeria). *International Journal of Botany Studies* 1(3): 3-7.

Deghiche-Diab, N. and Deghiche, L. 2019. *Flore adventice des oasis des Ziban. Biskra-Algeria*. Edition INRAA.150 p.

Deghiche-Diab, N. 2020. *Entomofaune des habitats humides, steppiques et phoenicicoles des Ziban: Approche structurale et fonctionnelle* (Doctoral dissertation, Université Mohamed Khider de Biskra).194p.

Deghiche-Diab, N. and Deghiche, T. 2022. New records and checklist of arthropods from two oasis ecosystems in Algeria. *Studia Universitatis Babeş-Bolyai Biologia*. 67(1): 89-105.

doi:10.24193/subbbiol.2022.1.05

Deghiche-Diab, N., Bologna, M.A., Boultif, M., Deghiche, T. and Boukerker, H. 2023. Mylabrini diversity and host plants in a Saharan oasis ecosystem with an updated checklist of Meloidae from Algeria (Coleoptera). *Fragmenta Entomologica* 55(1). pp. 21–30.

doi:10.13133/2284-4880/1473

De la Cruz, A.C., Gil, P.M., Fernández-Cancio, Á., Minaya, M., Navarro-Cerrillo, R.M., Sánchez Salguero, R. and Grau, J.M. 2014. Defoliation triggered by climate-induced effects in Spanish ICP Forests monitoring plots. *Forest Ecology and Management* 331(9): 245-255.

doi:10.1016/j.foreco.2014.08.010

Direction Générale des Forêts (DGF) 2020. Fiche signalétique de la forêt domaniale de Santé des forêts: Maladies, insectes, accidents climatiques. Diagnostic et prévention. Forêt Zouagha.

Encinas-Valero, M., Esteban, R., Heres, A. M., Vivas, M., Fakhet, D., Aranjuelo, I., Solla, A., Moreno, G. and Curiel Yuste, J. 2022. Holm oak decline is determined by shifts in fine root phenotypic plasticity in response to belowground stress. *New Phytologist* 235(6): 2237-2251.

doi:10.1111/nph.18182

Fayech, D. and Tarhouni, J. 2021. Climate variability and its effect on normalized difference vegetation index (NDVI) using remote sensing in semi-arid area. *Modeling Earth Systems and Environment* 7(3): 1667-1682.

doi:10.1007/s40808-020-00896-6

Fensholt, R., Langanke, T., Rasmussen, K., Reenberg, A., Prince, S.D., Tucker, C., … Wessels, K. 2012. Greenness in semi-arid areas across the globe 1981–2007-An Earth observing satellite based analysis of trends and drivers. *Remote Sensing of Environment* 121: 144-158.

doi:10.1016/j.rse.2012.01.017

Geist, H.J. and Lambin, E.F. 2004. Dynamic causal patterns of desertification. *BioScience* 54(9): 817-829.

doi:10.1641/0006-3568(2004)054[0817:DCPOD]2.0.CO;2

Gidey, E., Dikinya, O., Sebego, R., Segosebe, E. and Zenebe, A. 2018. Analysis of the long-term agricultural drought onset, cessation, duration, frequency, severity and spatial extent using vegetation health index (VHI) in Raya and its environs, Northern Ethiopia. *Environmental Systems Research* 7(13):

doi:10.1186/s40068-018-0115-z

Gitelson, A.A., Kaufman, Y.J. and Merzlyak, M.N. 1996. Use of a green channel in remote sensing of global vegetation from EOS-MODIS. *Remote Sensing of Environment* 58(3): 289-298.

doi:10.1016/S0034-4257(96)00072-7

Gorelick, N., Hancher, M., Dixon, M., Ilyushchenko, S., Thau, D. and Moore, R. 2017. Google Earth Engine: Planetary-scale geospatial analysis for everyone. *Remote Sensing of Environment* 202:18-27.

doi:10.1016/j.rse.2017.06.031

Hamlât, A., Kadri, C.B., Guidoum, A. and Bekkaye, H. 2021. Flood hazard areas assessment at a regional scale in M'zi wadi basin, Algeria. *Journal of African Earth Science* 182: 104281.

doi:10.1016/j.jafrearsci.2021.104281

Hersbach, H., Bell, B., Berrisford, P., Hirahara, S., Horányi, A., Muñoz-Sabater, J., … Thépaut, J.-N. 2020. The ERA5 global reanalysis. Quarterly *Journal of the Royal Meteorological Society* 146(730): 1999-2049.

doi:10.1002/qj.3803

Huete, A.R. 1988. A soil-adjusted vegetation index (SAVI). *Remote sensing of Environment* 25(3): 295-309.

doi:10.1016/0034-4257(88)90106-X

IPBES, 2018. The IPBES Assessment Report on Land Degradation and Restoration (Eds. L. Montanarella, R. Scholes and A. Brainich). Secretariat of the Intergovernmental Science-Policy Platform on Biodiversity and Ecosystem Services, Bonn, Germany, 744 p.

doi:10.5281/zenodo.3237392

IPCC 2021. Climate Change 2021: The Physical Science Basis. Contribution of Working Group I to the Sixth Assessment Report of the Intergovernmental Panel on Climate Change. Cambridge University Press, Cambridge, United Kingdom and New York, NY, USA.

doi:10.1017/9781009157896

Kim, H.Y. 2015. Statistical notes for clinical researchers: Post-hoc multiple comparisons. *Restorative Dentistry and Endodontics* 40(2): 172-176.

doi:10.5395/ rde.2015.40.2.172

Lambin, E.F., Turner, B.L., Geist, H.J., Agbola, S.B., Angelsen, A., Bruce, J.W., Coomes, O.T., Dirzo, R., Fischer, G., Folke, C., George, P.S., Homewood, K., Imbernon, J., Leemans, R., Li, X., Moran, E.F., Mortimore, M., Ramakrishnan, P.S., Richards, J.F., Skånes, H., Steffen, W., Stone, G.D., Svedin, U., Veldkamp, T.A., Vogel, C. and Xu, J. 2001. The causes of land-use and land-cover change: Moving beyond the myths. *Global Environmental Change* 11(4): 261-269.

doi:10.1016/S0959-3780(01)00007-3

Liang, J., Chen, C., Song, Y., Sun, W. and Yang, G. 2023. Long-term mapping of land use and cover changes using Landsat images on the Google Earth Engine Cloud Platform in bay area - A case study of Hangzhou Bay, China. *Sustainable Horizons* 7: 100061.

doi:10.1016/j.horiz.2023.100061

Maestre, F.T., Eldridge, D.J., Soliveres, S., Kéfi, S., Delgado-Baquerizo, M., Bowker, M.A., García-Palacios, P., Gaitán, J., Gallardo, A., Lázaro, R. and Berdugo, M. 2022. Dryland ecosystem degradation reduces ecosystem multifunctionality worldwide. *Science* 375 (6582): 1102-1109.

doi:10.1126/science.abm0395

Mersha, E., Degefa, S., Argaw, M. and Mengist, W. 2024. Impact of land use land cover changes on ecosystem service values: *Implication for Landscape Management* 18(1): 61-85.

doi:10.2478/jlecol-2025-0004

Moreira, F., Catry, F., Duarte, I., Acácio, V. and Silva, J. 2009. A conceptual model of sprouting responses in relation to fire damage: An example with cork oak (Quercus suber L.) trees in Southern Portugal. *Plant Ecology* 201(1): 77-85.

doi:10.1007/s11258-008-9476-0

Mushtaq, A.G. and Asima, N. 2016. Determining the vegetation indices (NDVI) from Landsat 8 satellite data. *International Journal of Advance Research* (IJAR), 4(8): 1459-1463.

doi:10.21474/IJAR01/1348

Nadezhdina, N., Ferreira, M. I., Silva, R. and Pacheco, C.A. 2008. Seasonal variation of water uptake of a Quercus suber tree in Central Portugal. *Plant and Soil* 305: 105-119.

doi:10.1007/s11104-007-9398-y

Office National of Meteorology (ONM). 2022. Annual report on climatological data: Biskra region. Algiers, Algeria: Office National of Meteorology. ONM Publishing

Ozenda, P. 2004. *Flore et végétation du Sahara*. 3ième édition. Centre National de la Recherche Scientifique CNRS. Paris. 662 p.

Parmesan, C. and Yohe, G. 2003. A globally coherent fingerprint of climate change impacts across natural systems. *Nature* 42: 37-42.

doi:10.1038/nature01286

Pettorelli, N., Schulte to Bühne, H., Tulloch, A., Dubois, G., Macinnis-Ng, C., Queirós, A. M., … Wegmann, M. 2018. Satellite remote sensing of ecosystem functions: Opportunities, challenges and way forward. *Remote Sensing in Ecology and Conservation* 4(2): 71-93.

doi:10.1002/rse2.59

Qi, J., Chehbouni, A., Huete, A.R., Kerr, Y.H. and Sorooshian, S. 1994. A modified soil adjusted vegetation index. *Remote Sensing of Environment* 48(2): 119-126.

doi:10.1016/0034-4257(94)90134-1

Quézel, P. and Santa, S. 1962-1963. *Nouvelle flore de l'Algérie et des régions désertiques méridionales*. CNRS, Paris, 1185 p.

Rahimi, E. and Dong, P. 2025. The influence of spatial extent shape on Lst-Ndvi patterns: A Multi-scale perspective, *Journal of Landscap Ecology* 18(1): 114-126.

doi:10.2478/jlecol-2025-0007

Rahimi, E., Dong, P. and Ahmadzadeh, F. 2025. Iran's dam waterbodies: A 10-Year Trend Analysis (2013-2023). *Journal of Landscape Ecology* 18(1),101-113.

doi:10.2478/jlecol-2025-0006

Reynolds, J.F., Smith, D.M., Lambin, E.F., Turner, B.L. 2nd, Mortimore, M., Batterbury, S.P., Downing, T.E., Dowlatabadi, H., Fernández, R.J., Herrick, J.E., Huber-Sannwald, E., Jiang, H., Leemans, R., Lynam, T., Maestre, F.T., Ayarza, M. and Walker, B. 2007.Global desertification: building a science for dryland development. *Science* 316(5826): 847-51.

doi:10.1126/science.1131634. PMID: 17495163

Rondeaux, G., Steven, M. and Baret, F. 1996. Optimization of soil-adjusted vegetation indices. *Remote Sensing of Environment* 55(2): 95-107.

doi:10.1016/0034-4257(95)00186-7

Roy, D.P., Wulder, M.A., Loveland, T.R., Woodcock, C.E., Allen, R.G., Anderson, M.C., Helder, D., Irons, J.R., Johnson, D.M., Kennedy, R., Scambos, T.A., Schaaf, C.B., Schott, J.R., Sheng, Y., Vermote, E.F., Belward, A.S., Bindschadler, R., Cohen, W.B., Gao, F., Hipple, J.D., Hostert, P., Huntington, J., Justice, C.O., Kilic, A., Kovalskyy, V., Lee, Z.P., Lymburner, L., Masek, J.G., McCorkel, J., Shuai, Y., Trezza, R., Vogelmann, J., Wynne, R.H. and Zhu, Z. 2014. Landsat-8: Science and product vision for terrestrial global change research. *Remote Sensing of Environment* 145:154-172.

doi:10.1016/j.rse.2014.02.001

Ruxton, G.D. and Beauchamp, G. 2008. Time for some a priori thinking about post hoc testing. *Behavioral Ecology* 19(3): 690–693.

doi:10.1093/beheco/arn020

Salemkour, N., Chalabi, K., Farhi, Y. and Belhamra, M. 2012. Inventaire floristique de la région des Ziban. *Journal Algérien des Régions Arides* 9(1): 3-16

Sanchez-González, M., Stiti, B., Chaar, H. and Cañellas, I. 2010. Dynamic dominant height growth model for Spanish and Tunisian cork oak (*Quercus suber* L.) forests. *Forest Systems* 19(3): 285-298.

doi:10.5424/fs/2010193-8495

Tandjaoui, A.F., Kaddour, M., De Oto, L., Guerid, H. and Khodadadzadeh, M. 2025. Mapping and monitoring spatiotemporal desertification patterns in the arid transition zone of Algeria over the period 2002–2022. International *Journal of Applied Earth Observation and Geoinformation* 104799.

doi:10.1016/j.jag.2025.104799

Tiberi, R., Branco, M., Bracalini, M., Croci, F. and Panzavolta, T. 2016. Cork oak pests: A review of insect damage and management. *Annals of Forest Science*, 73: 219-232.

doi:10.1007/s13595-015-0534-1

Turner, W., Rondinini, C., Pettorelli, N., Mora, B., Leidner, A.K., Szantoi, Z., Buchanan, G., Dech, S., Dwyer, J., Herold, M., Koh, L.P., Leimgruber, P., Taubenboeck, H., Wegmann, M., Wikelski, M. and Woodcock C. 2015. Free and open-access satellite data are key to biodiversity conservation. *Biological Conservation* 182:173-176.

doi:10.1016/j.biocon.2014.11.048

Turner, W., Spector, S., Gardiner, N., Fladeland, M., Sterling, E. and Steininger, M. 2003. Remote sensing for biodiversity science and conservation. *Trends in Ecology and Evolution* 18(6): 306-314.

doi:10.1016/S0169-5347(03)00070-3

Wulder, M.A., Coops, N.C., Roy, D.P., White, J.C. and Hermosilla, T. 2018. Land cover 2.0. *International Journal of Remote Sensing* 39(12):4254-4284.

doi:10.1080/01431161.2018.1452075

Wu, B., Smith, W.K. and Zeng, H. 2024. Dryland Dynamics and Driving Forces. In: *Dryland Social-Ecological Systems in Changing Environments* (Eds. B. Fu and M. Stafford-Smith). Springer, *Singapore*.

doi:10.1007/978-981-99-9375-8_2

Xie, S., Liu, L., Zhang, X., Yang, J., Chen, X. and Gao, Y. 2019. Automatic landcover mapping using Landsat timeseries data based on Google Earth Engine. *Remote Sensing* 11(24): 3023.

doi:10.3390/rs11243023

Xue, J. and Su, B. 2017. Significant remote sensing vegetation indices: A review of developments and applications. *Journal of Sensors* 2017(1): 1353691.

doi:10.1155/2017/1353691

Zhu, Z., Piao, S., Myneni, R.B., Huang, M., Zeng, Z., Canadell, J.G., Ciais, P., Sitch, S., Friedlingstein, P., Arneth, A., Cao, C., Cheng, L., Kato, E., Koven, C., Li, Y., Lian, X., Liu, Y., Liu, R., Mao, J., Pan, Y., Peng, S., Peñuelas, J., Poulter, B., Pugh, T.A.M., Stocker, B.D., Viovy, N., Wang, X., Wang, Y., Xiao, Z., Yang, H., Zaehle, S. and Zeng, N. 2016. Greening of the Earth and its drivers. *Nature Climate Change* 6(8):791-795.

doi:10.1038/nclimate3004

Zhu, Z., Zhang, J., Yang, Z., Aljaddani, A. H., Cohen, W. B., and Qiu, S. 2020. Continuous monitoring of land disturbance based on Landsat time series. *Remote Sensing of Environment* 238: 111116.

doi: 10.10106/j.rse.2019.03.009

Zou, X., Zhu, S. and Mõttus, M. 2022. Estimation of canopy structure of field crops using Sentinel-2 bands with vegetation indices and machine learning algorithms. *Remote* Sensing 14: 2849.

doi:10.3390/rs14122849

About the Authors

Nacima Deghiche-Diab is Senior Researcher (MRA), Scientific & Technical Research Center on Arid Regions (CRSTRA), Biskra, Algeria. PhD-qualified Senior Researcher specializing in agricultural entomology, pest management, and bioresource valorization in arid ecosystems. Expert in arthropod diversity, biological control, and circular bioeconomy innovations. Academic background includes a PhD from the University of Biskra and a Master's from CIHEAM-IAM Bari. Highly active in managing international research projects, drafting patents, and publishing on sustainable palm grove agroecosystems, medicinal flora, and alternative poultry feed sources.Her research activities encompass multiple fields related to crop protection, agricultural entomology, and the inventory of host plant species within arid flora.

Saliha Abbas is Research Professor | Scientific & Technical Research Center for Arid Areas (CRSTRA), Algeria. PhD-qualified Research Professor at CRSTRA specializing in GIS, satellite remote sensing, and geospatial modeling for arid and semi-arid ecosystems. Expert in multi-temporal satellite analysis (Landsat, Sentinel, MODIS), land-use/land-cover change detection, vegetation dynamics, and urban sprawl modeling. Authored key publications in *GeoJournal*, *Persian Journal of Acarology*, and *Belgeo*. Highly skilled in ArcGIS, QGIS, Google Earth Engine, and multi-criteria decision modeling (AHP, SWOT) for environmental monitoring and territorial development.

Printed in December 2026